Bioorganic & Medicinal Chemistry Letters 21 (2011) 1376–1381

Contents lists available at ScienceDirect

Bioorganic & Medicinal Chemistry Letters

journal homepage: www.elsevier.com/locate/bmcl

The design and synthesis of novel *N*-hydroxyformamide inhibitors of ADAM-TS4 for the treatment of osteoarthritis

Chris De Savi [a,*], Andrew Pape [a], John G. Cumming [a], Attilla Ting [a], Peter D. Smith [a], Jeremy N. Burrows [a], Mark Mills [a], Chris Davies [a], Scott Lamont [a], David Milne [a], Calum Cook [a], Peter Moore [a], Yvonne Sawyer [a], Stefan Gerhardt [b]

[a] *Respiratory and Inflammation Research Area, AstraZeneca, Mereside, Alderley Park, Macclesfield, Cheshire SK10 4TG, UK*
[b] *Global Structural Chemistry, AstraZeneca, Mereside, Alderley Park, Macclesfield, Cheshire SK10 4TG, UK*

ARTICLE INFO

Article history:
Received 17 December 2010
Revised 8 January 2011
Accepted 10 January 2011
Available online 18 January 2011

Keywords:
ADAM-TS4
MMP-13
Reverse hydroxamates
Aggrecanases
Osteoarthritis
Cyp inhibition

ABSTRACT

Two series of *N*-hydroxyformamide inhibitors of ADAM-TS4 were identified from screening compounds previously synthesised as inhibitors of matrix metalloproteinase-13 (collagenase-3). Understanding of the binding mode of this class of compound using ADAM-TS1 as a structural surrogate has led to the discovery of potent and very selective inhibitors with favourable DMPK properties. Synthesis, structure–activity relationships, and strategies to improve selectivity and lower in vivo metabolic clearance are described.

Osteoarthritis (OA) is a chronic disease that results in progressive cartilage degradation which clinically leads to pain and joint dysfunction.[1,2] Currently, this disease affects more than 20 million patients in the United States and this number is expected to double by 2020, making OA one of the most common health problems in this country. It is estimated that up to 90% of people older than 75 are affected by OA and of these almost all have OA in the hands and a third in the knee. Current pharmacological treatment for arthritis is limited to steroidal and non-steroidal anti-inflammatory drugs (NSAIDS). Although these drugs provide symptomatic relief for pain and inflammation in arthritis, they have failed to modify the progression of the disease.[3,4] There is still a massive unmet medical need to develop disease modifying agents that reduce or reverse the cartilage destruction associated with OA. Cartilage is primarily constituted of chondrocytes and an extracellular matrix that consists of aggrecan, collagen and water. Collagen primarily renders tensile strength whilst aggrecan is responsible for providing the elasticity and compressibility associated with cartilage.[5] Aggrecan and type-II collagen are degraded by proteolytic enzymes that have elevated activity in osteoarthritic joints. 'Aggrecanase-1' (ADAM-TS4)[6] and 'Aggrecanase-2' (ADAM-TS5)[7] have been identified as the most likely members of the ADAMTS (a disintegrin and metalloproteinase with thrombospondin) family to be responsible for cartilage aggrecan degradation and are attractive drug targets for intervention in OA.[8,9] ADAM-TS5 is responsible for disease progression in a surgically-induced model of OA in mice[10] nonetheless the relative individual contributions of ADAM-TS4 and ADAM-TS5 proteases to cartilage pathology in human disease is not fully understood.[11] Collagenases are the primary enzymes associated with type-II collagen cleavage and MMP-13 (collagenase-3) preferentially cleaves type-II collagen. Matrix metalloproteinase inhibitors (MMPi's) have been studied for many years as possible drugs for prevention of cartilage degradation but their clinical use has been limited by severe musculoskeletal side effects commonly characterized by joint stiffness and pain.[12,13] Histopathalogical findings attributed to fibrodysplasia have been seen in dogs following inhibition with a selective MMPi.[14] Furthermore, it is widely believed that aggrecan cleavage precedes collagen cleavage in the disease state[15] which justifies the need to discover potent inhibitors of aggrecanases void of MMP activity.[16]

* Corresponding author. Tel.: +44 1509644844.
E-mail address: chris.desavi2@astrazeneca.com (C. De Savi).

0960-894X/$ - see front matter © 2011 Elsevier Ltd. All rights reserved.
doi:10.1016/j.bmcl.2011.01.036

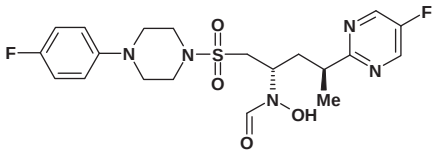

1

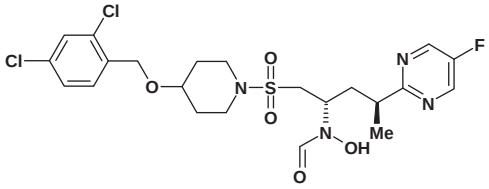

2

Two related series of *N*-hydroxyformamide inhibitors of ADAM-TS4, 'phenyl piperazines' represented by compound **1** and 'benzyloxypiperidines' represented by compound **2**, were identified from screening compounds previously synthesized as potential MMP-13 inhibitors.[17] Compound **1** was a potent inhibitor of ADAM-TS4 with acceptable physical, DMPK properties and hERG activity, but showed moderate inhibition of cytochrome P450 isoform 3A4. However the MMP selectivity profile was poor and moreover, SAR and structural studies (Table 1)[18,19] suggested that gaining the required selectivity within this sub-series would be very challenging. In contrast, benzyloxypiperidine **2** had poorer physical properties and hERG inhibition but a much better MMP selectivity profile. There appeared to be scope to address these issues by making changes to the substitution on the benzyl ring but all compounds suffered from potent cytochrome P450 isoform 3A4 inhibitory activity leading to concerns about potential drug–drug interaction.[20]

We hypothesised that increasing steric bulk around the *N*-hydroxyformamide moiety might disrupt its interaction with the cytochrome P450 haem group.[21] The fully substituted analogues, **3** and **4** were designed to test the hypothesis. The results show the addition of a methyl group adjacent to the *N*-hydroxyformamide does indeed reduce cytochrome P450 3A4 inhibitory activity (1.4 μM vs >10 μM, compounds **1** and **3,** respectively). A more dramatic improvement was observed for the benzyloxypiperidine series; highly potent cytochrome P450 3A4 inhibitors were transformed into a sub-series which were free of cytochrome P450 3A4 activity.

The ADME profile of di-substituted benzyloxypiperidine **4** was evaluated further and high metabolic liability was identified in both in vitro and in vivo systems; microsomal clearance in both human and rat was high, which was also observed in vivo in the rat with measured clearance (134 mL/min/kg) significantly in excess of hepatic liver blood flow. As a consequence short half life and low oral bioavailability were also observed. Non-radiolabelled metabolite identification studies suggested the major route of metabolism occurred via oxidation at the benzylic carbon atom. Furthermore cysteine conjugation adducts were also identified which indicated the presence of reactive metabolites. To address this, alternative linkers were proposed to replace the methyleneoxy group, using crystal structure information and modelling to rank the ideas (Table 2).[18,19]

A focused set of compounds were designed to improve the ADME properties of the benzyloxypiperidine series and CH_2CH_2 was identified as the optimal replacement linker. The new linker was tolerated when either piperidine or piperazine provided the central ring. Compounds **5** and **6** provide the direct piperazine and piperidine matched pair to compound **4**. Both compounds demonstrate maintained or improved aggrecanase potency, significantly reduced clearance, both in vitro and in vivo and acceptable bioavailability.

Previous attempts to generate crystal structures of our early inhibitors bound to ADAM-TS4 and ADAM-TS5 were unsuccessful, however a high quality structure of the surrogate enzyme ADAM-TS1, co-crystallised with inhibitors was obtained.[22] This surrogate system was used in conjunction with homology modeling of the ADAM-TS4 enzyme to (i) understand binding mode and key interactions, (ii) guide optimisation of MMP selectivity within the series, and (iii) rank proposed scaffold changes for likely ADAM-TS4 activity.

The focus of compound design now turned to modifying the substituents associated with the terminal phenyl ring of compound **6** to ultimately enhance cross-MMP isoform selectivity (Table 3). The single X-ray crystal structure of compound **4**, bound to the active site of ADAM-TS1 (Fig. 1a)[23] together with ADAM-TS4 homology model was used as the basis of a structure based design approach. Three key interactions were identified: (i) both oxygen atoms of the *N*-hydroxyformamide formed a chelate with the Zn^{2+} ion and additionally the formyl oxygen formed a hydrogen

Table 1
SAR for phenyl piperazine and benzyloxypiperidine compounds

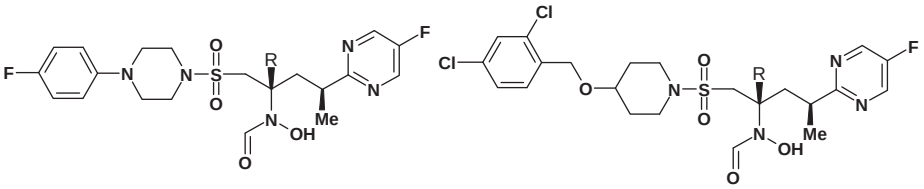

1 R = H
3 R = Me

2 R = H
4 R = Me

Compd	R	ADAM-TS4 IC_{50}[a] (nM)	MMP-1 IC_{50} (nM)	MMP-13 IC_{50} (nM)	MMP-14 IC_{50} (nM)	Cyp 3A4 IC_{50} (nM)	hERG IC_{50} (μM)
1	H	1.4	>1100	1.7	11	1.4	26
2	H	1	9700	1.6	180	<0.1	5
3	Me	7.3	980	60	7.6	>10	21
4	Me	3.5	>10,000	550	430	>10	8

[a] IC_{50}'s were derived from triplicate measurements whose standard errors were normally <5% in a given assay. Assay to assay variability was within twofold based on the results of a standard compound.

Table 2
Rat in vitro and in vivo data on alternative linkers

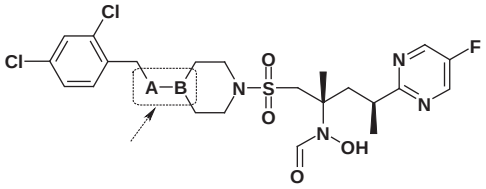

Compd	A	B	ADAM-TS4 IC_{50} (nM)	Hu Cl_{int}[a] (μL/min/mg)	Rat Cl_{int}[b] (μL/min/10^6 cells)	Cl[c] (mL/min/kg)	$t_{1/2}$ (h)	F[d] (%)
4	O	C	3.5	107	56.9	130	0.3	0
5	C	N	3.8	54	10.2	14	5.6	30
6	C	C	1.1	6.9	7.6	20	14.9	38
7	N	C	2200	nt	nt	nt	nt	nt

[a] Cl_{int} reported is mean of two separate experiments; nt = not tested.
[b] For procedure see Ref. 34.
[c] Compounds dosed at 2 mg/kg iv, $n = 2$ animals.
[d] Compounds dosed at 3–10 mg/kg po, $n = 4$ animals.

Table 3
Aggrecanase, MMP and ADAM inhibitory activities of piperidine ether analogs of **6**

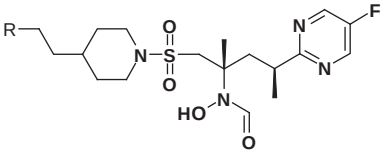

Compd	R	ADAM-TS4 IC_{50}[a] (nM)	MMP-1 IC_{50} (nM)	MMP-13 IC_{50} (nM)	MMP-14 IC_{50} (nM)	MMP-2 IC_{50} (nM)	TACE IC_{50} (nM)	$c \log P$
8a	2-Chloro-4-(trifluoromethyl)phenyl	0.48	>100,000	260	900	170	nt	4.9
8b	4-Chloro-2-methyl-phenyl	0.36	>8500	370	360	530	nt	4.5
8c	2-Bromo-4-fluoro-phenyl	0.48	>8000	2300	390	1700	nt	4.3
8d	2-Chloro-5-fluoro-phenyl	2.8	>9600	570	56	500	nt	4.2
8e	4-Fluoro-2-(trifluoromethyl)phenyl	0.52	9700	16,000	3600	1900	19	4.3
8f	3,5-Dimethylisoxazol-4-yl	0.69	>19,000	>8100	>8900	>6300	250	1.5
8g	4-Fluoro-2-methyl-phenyl	0.18	>8100	530	160	120	21	3.9
8h	2-Methyl-4-(trifluoromethyl)phenyl	0.49	>10,000	2300	4600	350	420	4.6
8i	2-Cyclopropyl-4-(trifluoromethyl)phenyl	0.94	>10,000	17,000	18,000	>9100	3200	5.1
8j	2,5-Dimethylphenyl	0.48	>10,000	23,000	4200	4200	22	4.3
8k	2,5-Dimethyl-4-pyridyl	0.43	>100,000	14,000	17,000	12,000	230	2.8
8l	2,5-Dimethyl-3-pyridyl	1.9	55,000	27,000	>8000	35,000	1400	2.8
8m	3,5-Dimethylisothiazol-4-yl	0.26	nt	4600	2600	2400	nt	2.9
8n	4,6-Dimethyl-3-pyridyl	0.68	>100,000	>4500	>3700	2200	3000	2.8
8o	3-Chloro-5-(trifluoromethyl)-2-pyridyl	4.2	>70,000	>16,000	>18,000	2800	27,000	3.6
8p	3-Methyl-5-(trifluoromethyl)-2-pyridyl	2.1	>79,000	6100	40,000	2500	24,000	3.3
8q	2-Chloro-4-methylsulfonyl-phenyl	0.57	>70,000	350	>3600	180	5500	2.5
8r	2,5-Dimethylpyrazol-3-yl	5.4	>10,000	6700	29,000	26,000	2800	1.5

[a] See footnote from Table 1.

bond interaction with Glu150, (ii) one of the sulfonyl group oxygens formed a hydrogen bond to the backbone NH of Leu118, and (iii) the 2,4-dichlorophenyl group was involved in a hydrophobic interaction with the residues forming the S1′ pocket. A further noteworthy feature of the observed binding model was the apparent stacked interaction between the fluoropyrimidinylmethyl P1 group and *N*-hydroxyformamide; the plane of the pyrimidine ring stacked parallel to the plane of the *N*-hydroxyformamide group. Further examination of the S1′ region of the crystal complex also indicated that the *ortho*-chloro atom associated with the 2,4-dichloro benzyl group occupied a small defined pocket of hydrophobic space. This particular finding was of significant interest as overlay with the single crystal X-ray structure of compound **4** in MMP-13 showed that this pocket did not appear to be present in MMP-13. This observation supported the exploration of further *ortho* -substituents in combination with a *para*-substituent, to define the SAR related to a potential increase in MMP selectivity. The importance of an *ortho*-substituted benzyl ether resulting in

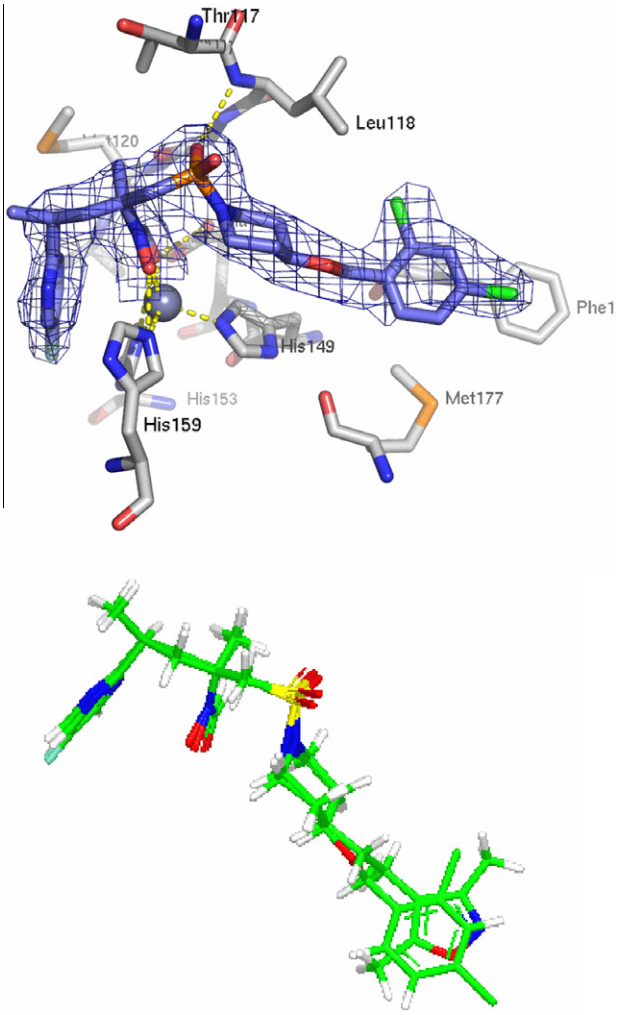

Figure 1. (a) ADAM-TS1 in complex with bound compound **4**. Key hydrogen bond interactions with active site residues of ADAM-TS1 are highlighted in yellow. The catalytic zinc ion (purple) is shown as a sphere. Final electron density map (blue mesh) is contoured at 1.0 s. (b) Overlay of bound compounds **4** and **8f** from ADAM-TS1 crystal structure complexes.

potent aggrecanase activity had also been noted on a series of 5-hydroxypipercolic hydroxamates from Noe et al.[24,25]

The overlaid conformations of bound compounds **4** and **8f** (Fig. 1b)[23] from ADAM-TS1 complexes gave the project team confidence both that the linker change would be tolerated and that the ortho methyl substituent associated with **8f** would access the exclusive ADAM- TS1 pocket.

All piperidine ether analogs (**8a**–**r**) exhibited excellent ADAM-TS4 potency in the picomolar to nanomolar range with excellent selectivity achieved compared with MMP-1. The majority of compounds also showed good selectivity compared with other MMPs. Small substituents such as F in the *meta* and *para* positions on the pendant aryl P1 group (compounds **8d** and **8g**) did not exhibit significant selectivity compared with MMP-14. The *ortho* Cl substituted compounds generally showed less selectivity towards both MMP-13 and MMP-2 (compounds **8a**, **8b**, 8d and **8q**). This interesting observation is further reinforced by comparing the nature of substituent in the ortho position where the *para* -substituent is fixed (**8a**, 8h and **8i**), and selectivity improves significantly for the *ortho* cyclopropyl variant (**8i**). Five membered heterocycles (**8f** and **8m**) in which both the *ortho* positions are flanked with methyl groups were both very potent ADAM-TS4 inhibitors and very selective across all measured MMPs (>5000-fold with respect to ADAM-TS4). The 2,5-dimethyl substitution pattern in particular inferred excellent MMP-13 selectivity as well as MMP-14 and MMP-1 (**8j**, 8k and **8l**). Generally, potency followed lipophilicity and the SAR was parallel between piperazine (**5**) and piperidine (**6**) sub-series, with the piperidine analogues showing two log units greater potency for most matched pairs (Fig. 2). Interestingly, although the pyridyl analogues (**8k**, **8l** and **8n**) followed the established *c* log *P* relationship, a number of the five-membered heterocycles showed a left-shifted relationship, that is, increased potency combined with reduced lipophilicity.

Due to the excellent selectivity profiles associated with **8f** it was taken forward for further in vitro and in vivo testing. The pharmacokinetic properties[26] in rat and dog showed low to moderate clearance (Cl_p = 11 and 20 mL/min/kg, respectively) and excellent half live ($t_{1/2}$ = 11 and 11.3 h) driven by good volume of distribution (V_{dss} = 7.4 and 9.2 L/kg). As a consequence of reduced lipophilicity, compound **8f** also demonstrated low plasma protein binding in rat (f_u = 0.22) and dog (f_u = 0.25). Oral bioavailability was moderate in dog (*F*% = 20) and mouse (*F*% = 34) and poor in rat (*F*% = 3.5%). However, upon higher oral dosing (50 and 100 mg/kg in DMSO/HP-β-CD formulation) AUC and bioavailability levels in rat increased significantly. Caco-2 data suggested good permeability with little efflux (Papp A:B = 5.3×10^{-6}; B:A = 10.9×10^{-6}). Compound **8f** also showed potent inhibition of IL-1 induced aggrecan (IC_{50} = 310 nM, n = 3) degradation in bovine nasal cartilage explants.[27] In human osteoarthritic cartilage, compound **8f** inhibited IL-1 induced aggrecan degradation with an IC_{50} = 243 nM.[28]

The synthesis of compound 8f is shown in Scheme 1. Chloropyrimidine **10** was synthesized via a Zn-mediated reduction using known literature methods from dichloropyrimidine **9**.[29] Compound **10** was subjected to a Pd mediated cyanation[30] followed by MeMgBr Grignard addition to the resultant nitrile to deliver methyl ketone **11** in 74% yield.

Ketone **11** smoothly underwent a Horner–Wadsworth–Emmons reaction to selectively deliver the cis α,β-unsaturated ketone **12** in 45% yield. The first chiral centre was introduced utilising an asymmetric hydrogenation using the 2*S*,5*S* (COD)Rh(EtDuPhos) catalyst with excellent control of stereochemistry to deliver **13**[31] in high yield (~88% ee, 90% yield). A Peterson reaction joined the chiral methyl ketone **13** with the pre-elaborated methanesulfonylpiperazine **14**,[32] and the resultant product was reacted in concert with hydroxylamine to generate the second, fully substituted chiral centre. Fortuitously the desired diastereoisomer was formed preferentially (2.2:1 major/minor diastereomeric ratio). Formylation of the hindered hydroxylamine **16** was achieved at room temperature following pre-formation of the *O*-acetyl derivative. After cleavage of the *O*-acetyl during work-up the desired diastereomer **8f**[33] crystallised with very high purity and diastereoisomeric excess. The route gave 4.9% overall yield with no chiral separation and has been used to synthesise >200 g of compound **8f** for early safety profiling.

In summary, we have discovered a very potent series of novel *N*-hydroxyformamide inhibitors of ADAM-TS4 with excellent selectivity over related metalloproteinases. The key issue of inhibition of cytochrome P450 was addressed by sterically hindering the metal-chelating group. Metabolic instability of the benzyloxy linker was addressed by replacement with an ethyl linker. Subsequent optimisation of the P1′ aryl group led to maintenance of potency with concomitant reduction of lipophilicity. A structure based design approach was supported with single crystal X-ray structures, using ADAM-TS1 as a structural surrogate. 3,5-Dimethloxazole **8f** showed excellent potency and selectivity combined with favourable DMPK properties and was advanced into in vivo safety studies and the guinea pig spontaneous OA PD model.

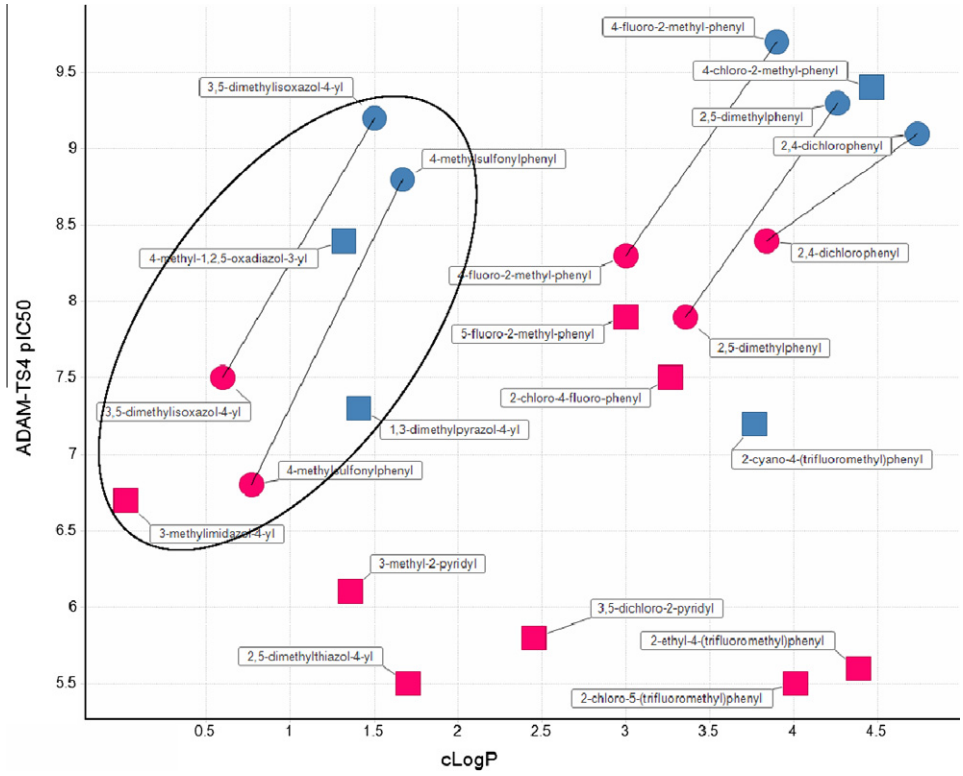

Figure 2. ADAM-TS4 potency versus *c* log *P*; SAR of aryl- and heteroaryl-ethyl piperidines (shown in blue) and ethyl piperazines (shown in red): region of more potency-lower lipophilicity (circled in black).

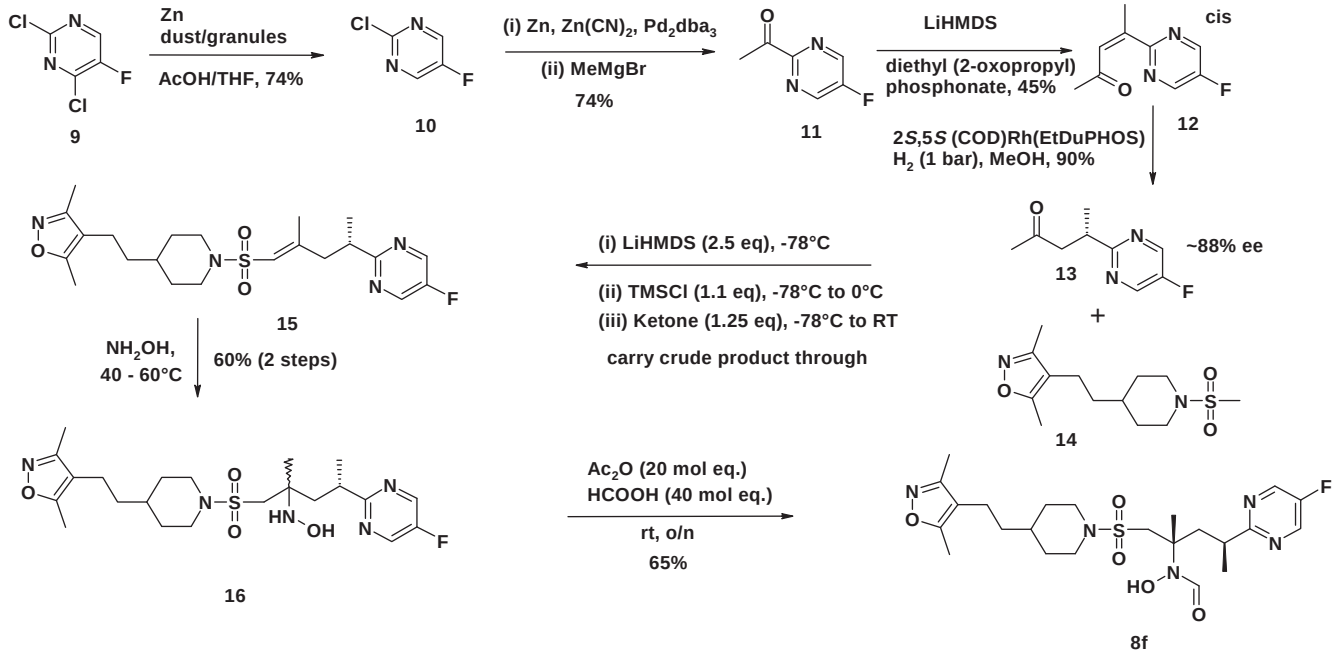

Scheme 1. Synthesis of *N*-hydroxyformamide oxazole **8f**.

Acknowledgements

We would like to acknowledge Mark W. M. Abbott and Paul Hawtin for construct design, Liz Flavell for molecular biology/purification and David Hargreaves for crystallisation and depositing structures into the RCSB protein data bank. We would also like to thank Mouloud Dekhane for his early explorations towards the synthesis of di-substituted reverse hydroxamates.

References and notes

1. Martel-Pelletier, J. *Osteoarthritis Cartilage* **1999**, *7*, 371.
2. Glodring, M. B.; Glodring, S. R. *J. Cell. Physiol.* **2007**, *213*, 626.
3. Fajardo, M.; Di Cesare, P. E. *Drugs Aging* **2005**, *22*, 141.
4. Singh, G. *Surg. Technol. Int.* **2003**, *11*, 287.
5. Kiani, C.; Chen, L.; Wu, Y. J.; Yee, A. J.; Yang, B. B. *Cell Res.* **2002**, *12*, 19.
6. Tortorella, M. D.; Burn, T. C.; Pratta, M. A.; Abbaszade, I.; Hollis, J. M.; Liu, R.; Rosenfeld, S. A.; Copeland, R. A.; Decicco, C. P.; Wynn, R.; Rockwell, A.; Yang, F.; Duke, J. L.; Solomon, K.; George, H.; Bruckner, R.; Nagase, H.; Itoh, Y.; Ellis, D.

M.; Ross, H.; Wiswall, B. H.; Murphy, K.; Hillman, M. C.; Hollis, G. F.; Newton, R. C.; Magolda, R. L.; Trzaskos, J. M.; Arner, E. C. *Science* **1999**, *284*, 1664.
7. Abbaszade, I.; Liu, R.-Q.; Yang, F.; Rosenfeld, S. A.; Ross, H.; Link, J. R.; Ellis, D. M.; Tortorella, M. D.; Pratta, M. A.; Hollis, J. M.; Wynn, R.; Duke, J. L.; George, H. J.; Hillman, M. C.; Murphy, K.; Wiswall, B. H.; Copeland, R. A.; Decicco, C. P.; Bruckner, R.; Nagase, H.; Itoh, Y.; Newton, R. C.; Magolda, R. L.; Trzaskos, J. M.; Hollis, G. F.; Arner, E. C.; Burn, T. C. *J. Biol. Chem.* **1999**, *274*, 23443.
8. Liu, R.-Q.; Trzaskos, J. M. *Curr. Med. Chem. Anti Inflamm. Anti Allergy Agents* **2005**, *4*, 251.
9. De Rienzo, F.; Saxena, P.; Filomia, F.; Caselli, G.; Colace, F.; Stasi, L.; Giordani, A.; Menziani, M. *Curr. Med. Chem.* **2009**, *16*, 2395.
10. Glasson, S. S.; Askew, R.; Sheppard, B.; Carito, B.; Blanchet, T.; Ma, H.-L.; Flannery, C. R.; Peluso, D.; Kanki, K.; Yang, Z.; Majumdar, M. K.; Morris, E. A. *Nature* **2005**, *434*, 644.
11. Stanton, H.; Rogerson, F. M.; East, C. J.; Golub, S. B.; Lawlor, K. E.; Meeker, C. T.; Little, C. B.; Last, K.; Farmer, P. J.; Campbell, I. K.; Fourie, A. M.; Fosang, A. J. *Nature* **2005**, *434*, 648.
12. Bigg, H. F.; Rowan, A. D. *Curr. Opin. Pharmacol.* **2001**, *1*, 314.
13. Brown, P. D. *Expert Opin. Invest. Drugs* **2000**, *9*, 2167.
14. Westwood, R.; Scott, R. C.; Somers, R. L.; Coulson, M.; Maciewicz, R. A. *Toxicol. Pathol.* **2009**, *37*, 860.
15. Pratta, M. A.; Yao, W.; Decicco, C.; Tortorella, M. D.; Liu, R.-Q.; Copeland, R. A.; Magolda, R.; Newton, R. C.; Trzaskos, J. M.; Arner, E. C. *J. Biol. Chem.* **2003**, *46*, 45539.
16. For a recent review of Aggrecanase inhibitors see: Gilbert, A. M.; Bikker, J. A.; O'Neil, S. V. *Expert Opin. Ther. Patents* **2011**, *21*, 1.
17. Barlaam, B. C.; Dowell, R. I.; Finlay, M. R. V.; Newcombe, N.; Tucker, H.; Waterson, D. WO 01/062742, 2001; *Chem. Abstr.* **2001**, *135*, 211053.
18. In vitro fluorescent assay for ADAM-TS4 inhibitors: Full length recombinant ADAM-TS4 proteases may be expressed and purified as described in Ref. 6. Using black 384 well plates, purified ADAM-TS4 (1.6 nM final) was incubated for 16 h at 37 °C in assay buffer (50 mM Hepes pH 7.5, 100 mM NaCl, 5 mM $CaCl_2$, 0.1% CHAPS, 5% glycerol) containing 25 μM synthetic substrate Abz-TEGEARGSVI-Dap(Dnp)-KK-NH (Anaspec, ANA60431-1) in the presence or absence of inhibitor (ranging from 10 μM to 0.036 nM). Cleavage of the substrate by ADAM-TS4 resulted in an increased fluorescence measured at λ_{ex} 340 nm and λ_{em} 420 nm. Compounds inhibiting this activity resulted in reduced fluorescence. An IC_{50} value for the inhibitor was calculated by plotting the raw data in a dose response curve fitting application (e.g., Origin).
19. In vitro fluorescent assay for matrix metalloproteinase family including for example MMP-13: Recombinant human proMMP-13 may be expressed and purified as described by Knauper et al. [Knauper, V., et al., *Biochem. J.* **1996**, *271*, 1544]. The purified enzyme was used to monitor inhibitors of activity as follows: purified proMMP-13 was activated using 1 mM amino phenyl mercuric acid (APMA) for 20 h at 35 °C in assay buffer (0.1 M Tris–HCl, pH7.5, containing 0.1 M NaCl, 20 mM $CaCl_2$, 0.02 mM ZnCl and 0.05% (w/v) brij 35 containing the synthetic substrate Mca-Pro-β-cyclohexyl-Ala-Gly-Nva-His-Ala-Dap(Dnp)-NH_2 (Bachem) in the presence or absence of inhibitors. Activity was determined by measuring the fluorescence at λ_{ex} 328 nm and λ_{em} 393 nm. An IC_{50} value for the inhibitor was calculated by plotting the raw data in a dose response curve fitting application (e.g., Origin). A similar protocol with the above substrate was used for expressed and purified pro MMP-1, -2, -3, -7, -8, -9, -14 and for MMP-19 the substrate Mca-Pro-Leu-Ala-Nva-Dpa-Ala-Arg-NH_2 (Bachem) was used. Similar protocols were applied for measuring the activity of ADAM-17 and ADAM-10 using the substrate Dimethoxyfluorescein-Ser-Pro-Leu-Ala-Gln-Ala-Val-Arg-ser-Ser-Arg-Cys-fluorescein (Bachem).
20. Zhou, S.; Yung, C. S.; Cher, G. B.; Chan, E.; Duan, W.; Huang, M.; McLeod, H. L. *Clin. Pharmacokinet.* **2005**, *44*, 279.
21. Williams, P. A.; Cosme, J.; Vinkovic, D. M.; Ward, A.; Angove, H. C.; Day, P. J.; Vonrhein, C.; Tickle, I. J.; Jhoti, H. *Science* **2004**, *305*, 683.
22. Gerhardt, S.; Hassall, G.; Hawtin, P.; McCall, E.; Flavell, L.; Minshull, C.; Hargreaves, D.; Ting, A.; Pauptit, R. A.; Parker, A. E.; Abbott, W. M. *J. Mol. Biol.* **2007**, *373*, 891.
23. The X-ray crystal ligand–protein structures of both compounds **4** (PDB ID = **3Q2G**) and **8f** (PDB ID = **3Q2H**) have been deposited into the RCSB Protein data bank (http://www.pdb.org/pdb/home/home.do).
24. Noe, M. C.; Natarajan, V.; Snow, S. L.; Mitchell, P. G.; Lopresti-Morrow, L. L.; Reeves, L. M.; Yocum, S. A.; Carty, T. J.; Barberia, J. T.; Sweeney, F. J.; Liras, J. L.; Vaughn, M.; Hardink, J.; Hawkins, J. M.; Tokar, C. *Bioorg. Med. Chem. Lett.* **2005**, *15*, 2808.
25. Noe, M. C.; Natarajan, V.; Snow, S. L.; Wolf-Gouveia, L. A.; Mitchell, P. G.; Lopresti-Morrow, L.; Reeves, L. M.; Yocum, S. A.; Carty, T. J.; Otterness, I.; Bliven, M. A.; Carty, T. J.; Barberia, J. T.; Sweeney, F. J.; Liras, J. L.; Vaughn, M. *Bioorg. Med. Chem. Lett.* **2005**, *15*, 3385.
26. Male and female Han Wistar rats and Beagle dogs were obtained from in-house colonies. Doses administered by the iv route were delivered to rats as a solution in 40% aq dimethylamide (2 mg/kg) and to dogs in 5% DMSO/95% Sorensen's buffer, pH5.5 (1 mg/kg), while those administered by the oral route were delivered to rats in 10% DMSO/90% aq hydroxypropyl methylcellulose/Tween and to dogs in 5% DMSO/95% aq hydroxypropyl methylcellulose/Tween. Blood samples (50–200 μL) were collected from the tail vein of rats (t = 5, 20 and 40 min, 1.5, 3, 6, 12, and 24 h and 15 and 30 min, 1, 2, 3, 6, 12 and 24 h following iv and oral administration, respectively) and the jugular vein of dogs (t = 5, 10, 20 and 40 min, 1, 2, 4, 6, 12, 24, 36 and 48 h and 10, 20 and 40 min, 1, 2, 3, 4, 6, 12, 24, 36 and 48 h following iv and oral administration, respectively). Blood was diluted with an equal volume of water and a 50 μL aliquot of the diluted sample was extracted by precipitation with 150 μL ice-cold acetonitrile. Drug levels were determined by LC–MS/MS analysis. Pharmacokinetic parameters were calculated using the non-compartmental method in Win-Nonlin v2.1 (Pharsight, Mountain View, CA).
27. Bovine Cartilage Explant Culture Natural Substrate Assay: The activity of the compounds as inhibitors of aggrecan degradation in cartilage explant cultures may be assayed by measuring the inhibition of released aggrecan fragments for example based on the disclosures of Arner, E.C., et al. *Osteoarthritis Cartilage* **1998**, *6*, 214. Cartilage discs (5 × 2 mm) were dissected from bovine nasal cartilage and each disc was cultured in a well of a 96-well plate containing 200 μL Dulbecco's Modified Eagle's Medium (DMEM, Sigma) containing 100 U/mL of penicillin, 100 μg/mL of streptomycin, 8 mM L-glutamine and 2.5 μg/mL amphotericin B. The plates were incubated at 37 °C in 5% CO_2 environment. After a recovery phase of 3 days the media was changed to media containing 10 ng/mL IL-1α (R&D Systems) plus a range of inhibitor concentrations. Control samples containing no IL-1α were included. After 48 h the media was analysed for aggrecanase activity by immobilising the protein onto nitrocellulose membrane using dot blot apparatus followed by immunodetection of the neo-epitope NITEGE using a specific anti-NITEGE primary antibody. Quantification was achieved by using an anti-rabbit-HRP secondary antibody and a chemiluminescent substrate (ECL, Amersham). The blots were read on a Packard luminescence counter. An IC_{50} value for the inhibitor was calculated by plotting the raw data in a dose response curve fitting application (e.g., Origin).
28. Human knee cartilage was obtained at the time of knee replacement surgery or from cadavers. Cartilage was placed in culture and stimulated for 5 days with IL-1 plus Oncostatin M. Aggrecanase activity was measured as for the bovine cultures and a good correlation between the human and bovine systems has been established.
29. Dunaiskis, A.; Staigers, T.; Keltonic, T.; Chappie, T.; Meltz, C.; Dugger, R.; Sanner, M. A. *Org. Prep. Proc. Int.* **1995**, *27*, 600.
30. Jin, F.; Confalone, P. N. *Tetrahedron Lett.* **2000**, *41*, 3271.
31. Selected experimental and analytical information: Compound **13**: (4*S*)-4-(5-fluoropyrimidin-2-yl)pentan-2-one: (*E*)-4-(5-fluoro-pyrimidin-2-yl)-pent-3-en-2-one (50 g, 27.7 mmol) and (1,2-bis((2*S*,5*S*)-2,5-diethylphospholano)-benzene)(1,5-cyclooctadiene)rhodium(I)tetrafluoroborate (0.0130 equiv) in methanol (500 mL) were stirred at 20 °C under an atmosphere of hydrogen at 1 bar and for 3 h. The catalyst was removed by filtration and the filtrate was concentrated under reduced pressure. The residue was dissolved in diethyl ether (150 mL) and the precipitate was removed by filtration. The filtrate was concentrated under reduced pressure. The ensuing residue was subjected to flash chromatography (silica, 40% ethyl acetate/hexanes) and concentration of the appropriate fractions afforded **13** (49.6 g, 96%) as a pale yellow oil. The product was 86% ee, as assessed by analytical chiral chromatography; ^{1}H NMR spectrum: (400.13 MHz, $CDCl_3$) δ 1.32 (3H, d), 2.17 (3H, s), 2.68–2.73 (1H, m), 3.17–3.23 (1H, m), 3.61–3.67 (1H, m), 8.51 (2H, s); Mass spectrum: LRMS (APCI) m/z $[M+H]^+$ 183.
32. Selected experimental and analytical information: Compound **14**: 3,5-dimethyl-4-{2-[1-(methylsulfonyl)piperidin-4-yl]ethyl}isoxazole: 4-[(*E*)-2-(3,5-dimethyl-1,2-oxazol-4-yl)ethenyl]-1-(methylsulfonyl)piperidine (3.1 g, 10.9 mmol) and palladium, 10% on charcoal (catalytic) in ethanol (60 mL) were stirred under an atmosphere of hydrogen at 20 °C for 16 h. The catalyst was removed by filtration and the filtrates were concentrated under reduced pressure to give **14** (3.1 g, 98%) as a white solid; ^{1}H NMR (400.13 MHz, $CDCl_3$) 1.33–1.46 (5H, m), 1.82–1.84 (2H, m), 2.20(3H, s), 2.30–2.33(5H, m), 2.62 (2H, m), 2.78 (3H, s), 3.82 (2H, d); Mass spectrum: LRMS (APC I) m/z $[M+H]^+$ 287.
33. Selected experimental and analytical information: Compound **8f**: *N*-[(2*S*,4*S*)-1-({4-[2-(3,5-dimethyl-1,2-oxazol-4-yl)ethyl]piperidin-1-yl}sulfonyl)-4-(5-fluoropyrimidin-2-yl)-2-methylpentan-2-yl]-*N*-hydroxyformamide; acetic anhydride (2020 mL, 21373 mmol) was added portion wise to a suspension of *N*-(1-(4-(2-(3,5-dimethylisoxazol-4-yl)ethyl)piperidin-1-ylsulfonyl)-4-(5-fluoropyrimidin-2-yl)-2-ethylpentan-2-yl)hydroxylamine (1010 g, 1526.7 mmol) in THF (7.5L) at 5 °C and was then stirred at 45 °C for 15 min. Formic acid (1613 mL, 42747 mmol) was then added portion wise at −5 °C and the reaction mixture was stirred at 10 °C for 2 h and then at 45 °C overnight. The mixture was concentrated under reduced pressure and azeotroped with toluene (2 × 1.25 L). The residue was dissolved in methanol (2.25 L), cooled to 10 °C and 7 N ammonia in methanol (2 L) was added over 20 min. The reaction mixture was stirred at 15 °C for 10 min and was then concentrated under reduced pressure. The residue was slurried in ethyl acetate (1 L and the precipitate which was formed was removed by filtration. The filtrate was concentrated under reduced pressure and the crude product was purified by prep HPLC (silica, elution gradient 10–80% ethyl acetate in isohexane). Fractions containing the desired compound were concentrated under reduced pressure and the residue was recrystallised from ethanol (3.5 L) to give **8f** (327 g, 41%) as a white solid. The required compound was isolated as a single diastereoisomer, Purity 98.3% @ 220 nm; Mass spectrum: LRMS (APCI) m/z $[M+H]^+$ 512; ^{1}H NMR (400.13 MHz, $CDCl_3$) δ 1.28–1.43 (7H, m), 1.77–1.85 (5H, m), 2.19 (3H, s), 2.27–2.31 (5H, m), 2.64–2.72 (3H, m), 3.06 (1H, d), 3.25–3.28 (1H, m), 3.40 (1H, d), 3.76 (2H, d), 8.01 (1H, s), 8.55 (2H, s); ^{13}C NMR (176 MHz, DMSO) δ 169.6, 164.2, 159.0, 156.0, 155.1, 144.7, 144.7, 113.3, 61.3, 52.7, 45.2, 45.2, 43.3, 37.3, 35.4, 33.9, 31.1, 31.1, 22.5, 18.3, 18.29, 10.4, 9.7; HRMS m/z $[M+H]^+$ 512.23364, calcd 512.23374, (err. 0.20 ppm); Melting point 138–142 °C; Elemental Anal. Calcd for $C_{23}H_{34}FN_5O_5S \cdot 0.05EtOH$, $1.35H_2O$: C, 53.3; H, 6.8; N, 13.5; F, 3.7; S, 6.2. Found: C, 53.6; H, 6.7; N, 3.8; F, 3.8; S, 6.2.
34. Houston, J. B.; Carlile, D. J. *Drug Metab. Rev.* **1997**, *29*, 891.